IMPLEMENTATION OF A PSEUDO-BENDING SEISMIC TRAVEL-TIME CALCULATOR IN A DISTRIBUTED PARALLEL COMPUTING ENVIRONMENT

Sandy Ballard, Chris Young, Jim Hipp, Glenn Barker, and Marcus Chang

Sandia National Laboratories

Sponsored by National Nuclear Security Administration

Contract No. DE-AC04-94AL8500

ABSTRACT

Pseudo-bending is an algorithm for calculating seismic travel time through complex 3D velocity models. The algorithm was originally proposed by Um and Thurber (1987) and later extended by Zhao et al. (1992) to account for first order velocity discontinuities. We have modified Zhao's method of handling discontinuities by implementing a two-dimensional (2D) minimization algorithm that searches for the point on the velocity discontinuity surface where Snell's Law is satisfied. Further, our implementation reduces the likelihood that the pseudo-bending algorithm will return a local minimum by starting the ray calculation from several different starting rays. Specifically, interfaces are defined that include first order discontinuities plus additional interfaces at levels of the model where local minima might be generated. Rays are computed that are constrained to bottom in each layer between these interfaces. The computed rays might be reflected off the top of the layer, turn within the layer, or diffract along the interface at the bottom of the layer. The computed ray that is seismologically valid and that has the shortest travel time is retained.

The modifications we have made to the algorithm have made it more accurate and robust but have also made it more computationally expensive. To mitigate this impact, we have implemented our software in a distributed parallel computing environment, which makes possible the calculation of many rays simultaneously.

Report Documentation Page

Form Approved
OMB No. 0704-0188

1. REPORT DATE	2. REPORT TYPE	3. DATES COVERED
SEP 2008		**00-00-2008 to 00-00-2008**

4. TITLE AND SUBTITLE	5a. CONTRACT NUMBER
Implementation of a Pseudo-Bending Seismic Travel-Time Calculator in a Distributed Parallel Computing Environment	5b. GRANT NUMBER
	5c. PROGRAM ELEMENT NUMBER
6. AUTHOR(S)	5d. PROJECT NUMBER
	5e. TASK NUMBER
	5f. WORK UNIT NUMBER
7. PERFORMING ORGANIZATION NAME(S) AND ADDRESS(ES) **Sandia National Laboratories,PO Box 969,Livermore,CA,94551-0969**	8. PERFORMING ORGANIZATION REPORT NUMBER
9. SPONSORING/MONITORING AGENCY NAME(S) AND ADDRESS(ES)	10. SPONSOR/MONITOR'S ACRONYM(S)
	11. SPONSOR/MONITOR'S REPORT NUMBER(S)

12. DISTRIBUTION/AVAILABILITY STATEMENT
Approved for public release; distribution unlimited

13. SUPPLEMENTARY NOTES
Proceedings of the 30th Monitoring Research Review: Ground-Based Nuclear Explosion Monitoring Technologies, 23-25 Sep 2008, Portsmouth, VA sponsored by the National Nuclear Security Administration (NNSA) and the Air Force Research Laboratory (AFRL)

14. ABSTRACT
see report

15. SUBJECT TERMS

16. SECURITY CLASSIFICATION OF:			17. LIMITATION OF ABSTRACT	18. NUMBER OF PAGES	19a. NAME OF RESPONSIBLE PERSON
a. REPORT **unclassified**	b. ABSTRACT **unclassified**	c. THIS PAGE **unclassified**	**Same as Report (SAR)**	**9**	

OBJECTIVE

Our goal is to develop a practical, accurate, infinite frequency travel-time calculator through three-dimensional (3D) models of the distribution of seismic velocity in the Earth.

RESEARCH ACCOMPLISHED

Background

Three-dimensional models of the velocity distribution within the Earth are becoming increasingly available in the seismological research community and have the potential to significantly improve our ability to accurately and precisely locate seismic events around the world (e.g,. Flanagan et al., 2007). These 3D models are generally derived directly from observed travel times, using tomographic inversion techniques. Development of these models and use of the models in seismic-event location calculations, requires the ability to accurately compute predicted source-to-receiver travel times though the proposed 3D velocity structures. This is a complicated and computationally expensive task, and the many algorithms that have been proposed to accomplish it fall into three broad categories. Eikonal solvers (e.g., Vidale, 1988, 1990; Podvin and Lecomte, 1991; Rawlinson and Sambridge, 2004a, 2004b; and deKool et al., 2006) employ finite-difference techniques to propagate wavefronts through 3D velocity distributions defined on a 3D grid of points, thereby computing predicted travel times between a single point and an entire grid of points distributed within the medium. Ray shooters (e.g., Menke) systematically perturb an initial estimate of the ray take-off angle from a seismic source until the ray hits the seismic receiver, within some prescribed tolerance. Ray benders (e.g., Um and Thurber, 1987) start with an initial estimate of the ray geometry connecting the source and receiver and perturb the geometry of the ray until Fermat's principle of stationary time is satisfied all along the ray path. Though very different in approach to the problem, all of these techniques assume that the wave propagates from source to receiver with infinite frequency.

After reviewing several available algorithms, we chose to implement a version of the ray-bending algorithm described by Um and Thurber (1987), which was extended to include the effects of velocity discontinuities by Zhao et al. (1992) and Koketsu and Sekine (1998). We considered this algorithm superior to finite-difference eiknonal solvers for our intended applications because it provides direct, point-to-point travel times without interpolation off a grid and because it does not require calculation of full volumes of travel times for a small number of source-receiver pairs. We also consider it to be superior to ray shooters in that it will always find a solution, even in the presence of low-velocity zones, which can cause ray shooters to fail.

The algorithm is based on the fact that, along a valid ray path, the ray curvature is proportional to the component of the local velocity gradient normal to the ray path (Figure 1). The algorithm steps along an initial estimate of the path, perturbing the center point (X_k in Figure 1) of three adjacent points on the path so that it satisfies this condition (X_k' in Figure 1). Zhao et al. (1992) and Koketsu and Sekine (1998) extended the algorithm to include the effects of planar and spherical velocity discontinuities, respectively. In this paper, we further extend the algorithm to allow discontinuities at arbitrary orientations. These modifications, described in detail in the next section, preclude the inclusion of the "enhancement factor" described by Um and Thurber (1987), and we have not included it in our implementation.

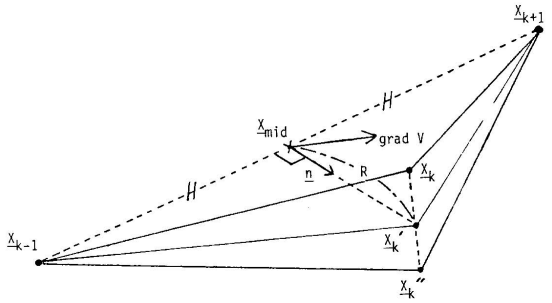

Figure 1. Pseudo-bending algorithm (from Um and Thurber, 1987).

A key feature of any system for computing travel time through 3D Earth models is the subsystem used to represent, and interpolate velocity values from, the 3D model itself. The system we use is described in detail in a companion paper (Ballard et al., 2008; these Proceedings) and is not reviewed here.

Velocity Discontinuities

Figure 2 depicts two media, M_1 and M_2, with velocity distributions $V_1(x, y, z)$ and $V_2(x, y, z)$, which may vary in three dimensions but which are first-order continuous internally. Surface S represents the smooth boundary between the two media such that the velocity may be discontinuous across S. The curve in Figure 2 represents the intersection of S with the plane of the figure, but S may dip into and/or out of the plane of the figure. Unit vector $\vec{n}$ is normal to S at X and does not necessarily lie in the plane of the figure. P_1 and P_2 are points in M_1 and M_2, respectively.; $\vec{x}_1$ and $\vec{x}_2$ are unit vectors that point from X toward P_1 and P_2 respectively.

In order for points P_1, X and P_2 to lie on a common ray path, Snell's Law must be honored at X, which requires that the following 3 conditions be satisfied:

$$C_1 = \frac{\sin\theta_1}{V_1} - \frac{\sin\theta_2}{V_2} = 0 \qquad (1)$$

$$C_2 = (\vec{x}_1 \times \vec{x}_2) \bullet \vec{n} = 0 \qquad (2)$$

and

$$C_3 = (\vec{x}_1 \times \vec{n}) \bullet (\vec{x}_2 \times \vec{n}) \le 0\,. \qquad (3)$$

In Equation 1, V_i , i=1,2 is the arithmetic average of the velocity at P_i and the velocity at X on the same side of S as P_i. Equation 2 requires that, $\vec{x}_1$, $\vec{x}_2$, and $\vec{n}$ be coplanar, implying that $\vec{n}$ lies in the plane of Figure 2 when Snell's Law is satisfied. Equation 3 prohibits $\vec{x}_1$ and $\vec{x}_2$ from residing on the same side of the line containing $\vec{n}$ (i.e., a nonphysical ray path). Figure 3 (a,b, and c) illustrates example distributions of Equations 1 through 3 displayed on a projection of S onto a spherical cap that passes through X.

While ray tracing, we are given points P_1 and P_2 on opposite sides of S and seek point X on S that satisfies Snell's Law, as expressed by the three conditions above. To find X, we implement a 2D search algorithm that minimizes

$$F = |C_1| + |C_2| + 10|C_3|\,. \qquad (4)$$

Experience indicates that the factor of 10 applied to C_3 improves convergence behavior. Figure 3d illustrates an example distribution of F on a projection of S onto a spherical cap that passes through X.

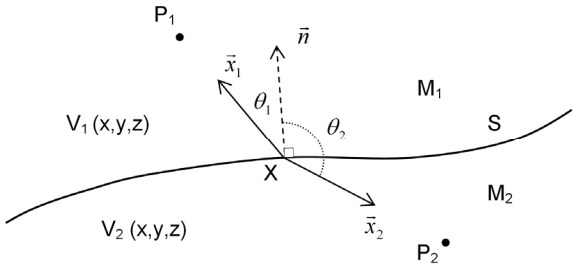

Figure 2. Snell's Law applied at point X on surface S.

Phase Discrimination

A problem that frequently arises when using the bending algorithm to predict travel times through realistic, regional to teleseismic scale, 3D models is that there exists more than one valid ray that connects a given source-receiver pair (Figure 4). Some of these rays represent different seismic phases, but even for a single phase there can be multiple valid rays that bottom at different levels in the Earth. Each of these represents a local minimum travel time but only once can represent the overall minimum path. To ensure that we get the desired ray, we specify a number of interfaces within the Earth and require the bender to compute rays that are constrained to bottom in each of the layers defined by those interfaces. We specify interfaces at all the velocity discontinuities with which a ray of a given phase must interact (Moho, 410, 660, etc.). We specify additional interfaces at levels within the Earth model that could potentially generate travel-time triplications, even though the velocity is continuous across these interfaces. The ray computed for each layer might be one that refracts within the layer, reflects off the interface at the top of the layer, or diffracts along the interfaces at the top and/or bottom of the layer.

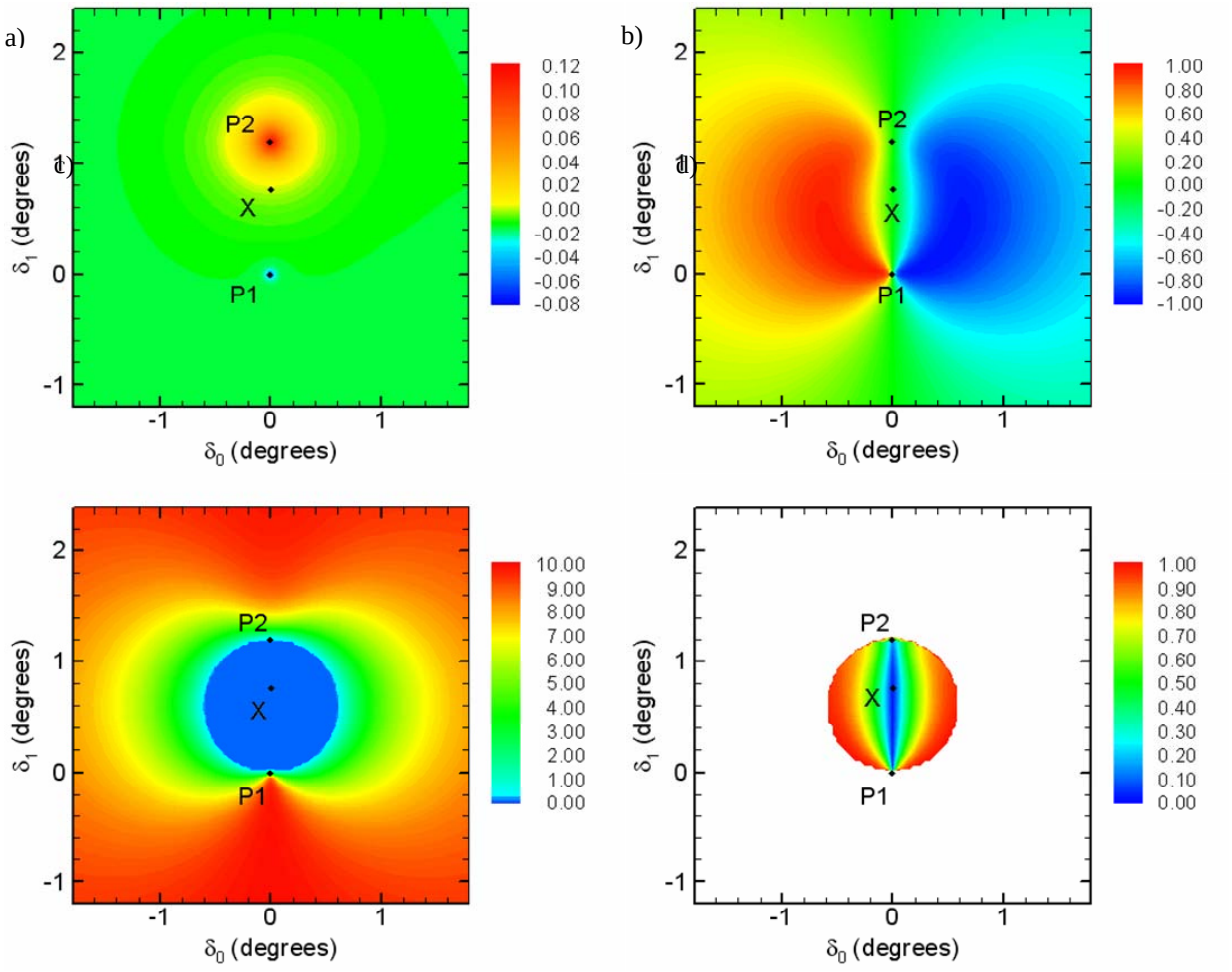

Figure 3. Plots of (a) Equation 1, (b) Equation 2, (c) Equation 3, and (d) Equation 4 displayed on a projection of S onto a spherical cap that passes through X. Points P1 and P2 lie above and below the plane of the figures, respectively. In (d), portions of the map where Equation 3 is not equal to zero are blanked out.

Not all of these rays are valid and hence can be discarded. In particular, rays that reflect off of, or diffract along, defined interfaces across which the velocity is continuous are not valid. If more than one valid ray is calculated from a given set of defined interfaces, the ray with the shortest travel time is retained.

A further advantage of this approach is that travel time for any desired phase can be computed by specifying the interfaces in the Earth with which the ray must interact (Figure 5). For example, to compute predictions for phase Pn, one would specify only the Moho and other interfaces in the mantle down to, but not including, the 660-km discontinuity, thereby constraining the computed ray to bottom somewhere in the mantle above the 660.

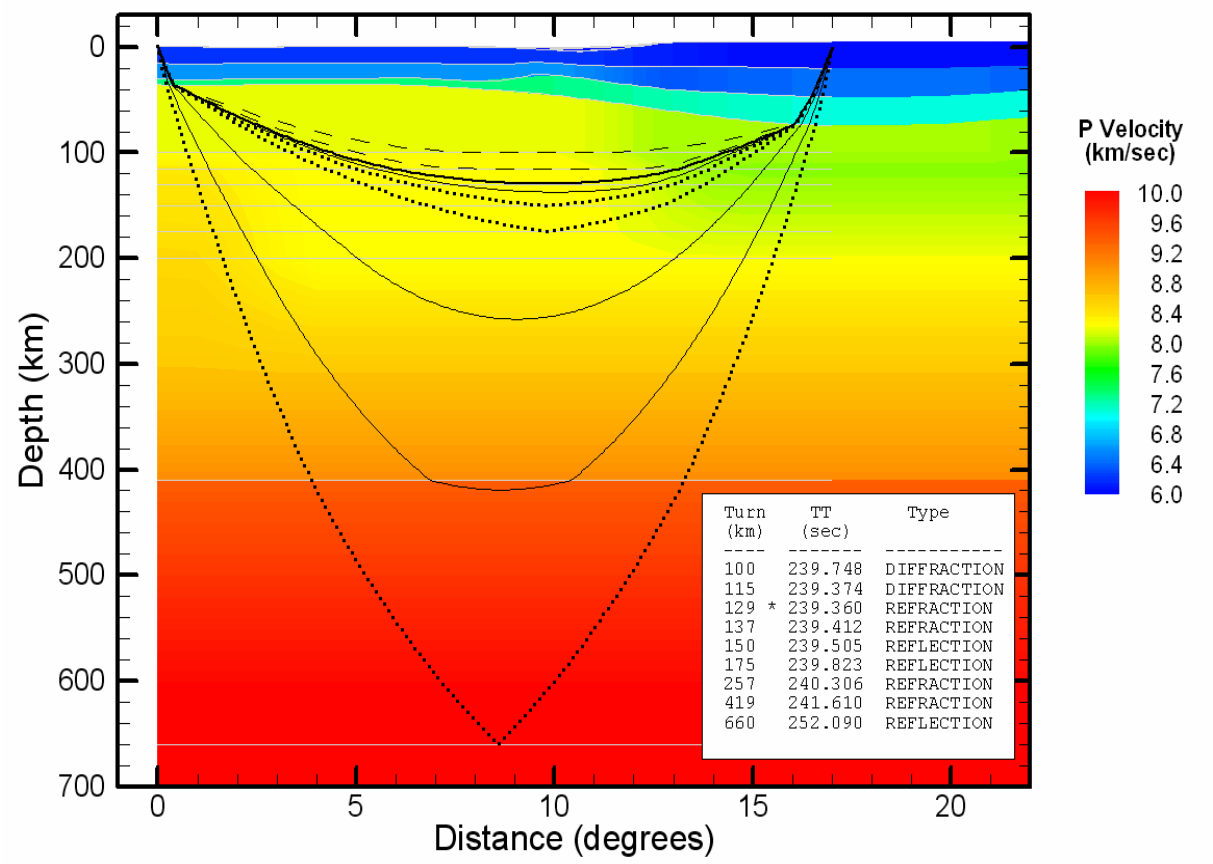

Figure 4. Multiple valid seismic rays connect a given source and receiver, each constrained to bottom in a specified layer of the Earth model.

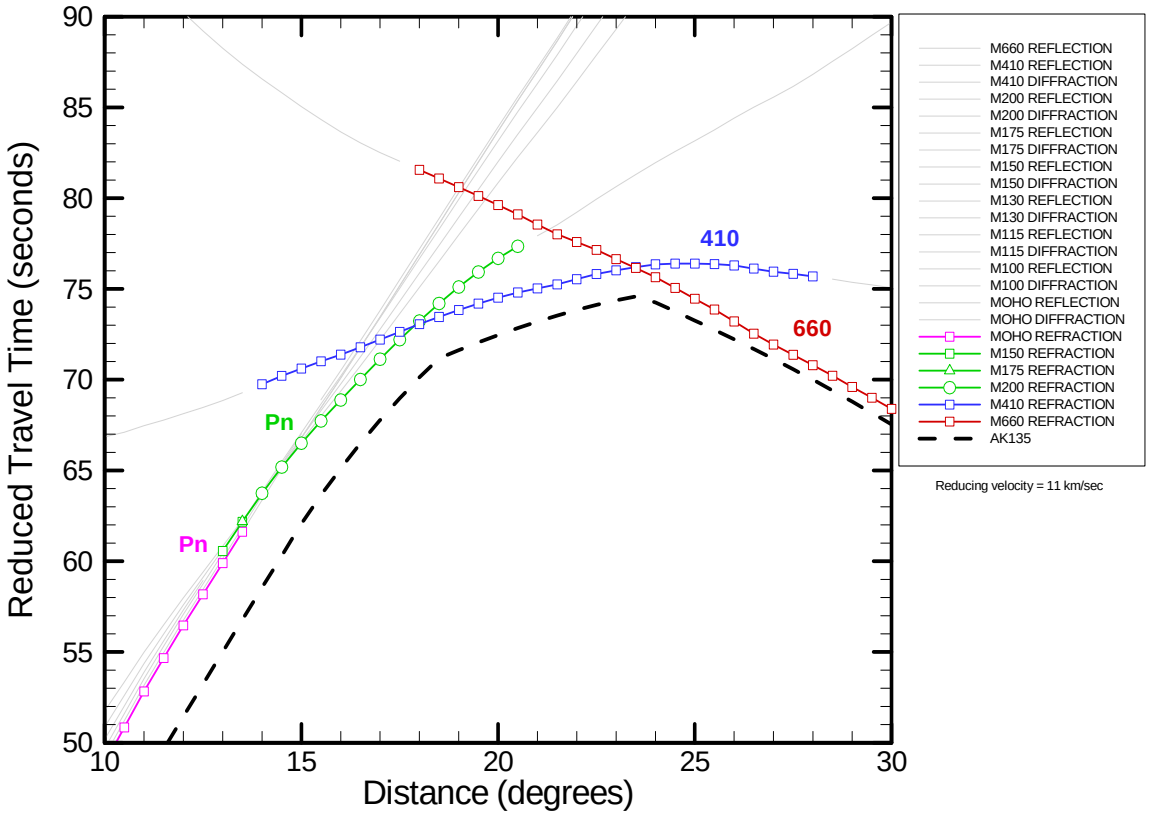

Figure 5. Travel-time curves for a source-receiver pair in a 3D Earth model with velocity generally less than that of the AK135 model.

Algorithm Verification

We have verified the validity of the bender algorithm in two ways. First, we constructed a 3D version of the radially symmetric AK135 model (Kennett et al., 1995). The 3D version is deployed on a uniform, 1° triangular tessellation similar to the tessellations we use for more-complex 3D models (Ballard et al., 2008; these Proceedings), but the model is based on a spherical Earth with the same velocity discontinuities and radial velocity distribution as the AK135 model. Rays through the model computed with Bender are shown in Figure 6, and travel times computed with Bender and using the TaupToolkit software (Crotwell et al., 1999) are compared in Figure 7. The difference at all regional and teleseismic distances is at most a few hundredths of seconds, indicating that Bender is very accurate, even for long path lengths.

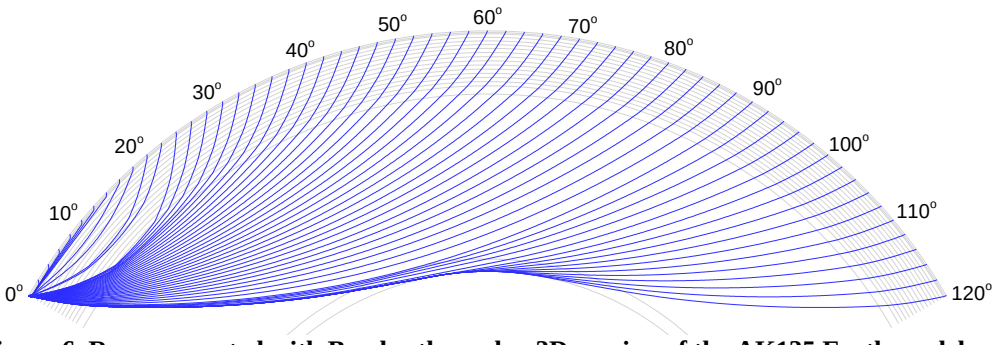

Figure 6. Rays computed with Bender through a 3D version of the AK135 Earth model.

To verify the validity of Bender travel times through Earth models with significant 3D velocity variations, we built a 3D model based on the a priori GNEMRD Unified Model (Begnaud et al., 2004; Pasyanos et al., 2004) and computed travel times through it using our Bender code and the FMM code (De Kool et al., 2006). Topography and bathymetry for the Unified Model were derived from ETOPO5, while shallow sedimentary layers were taken from the 1-degree-resolution sediment model of Laske and Masters (1997). The structure of crust and uppermost mantle is drawn from a variety of focused regional studies. The upper-mantle model (below 100 km) is taken from the a priori 3SMAC model (Nataf and Ricard, 1996).

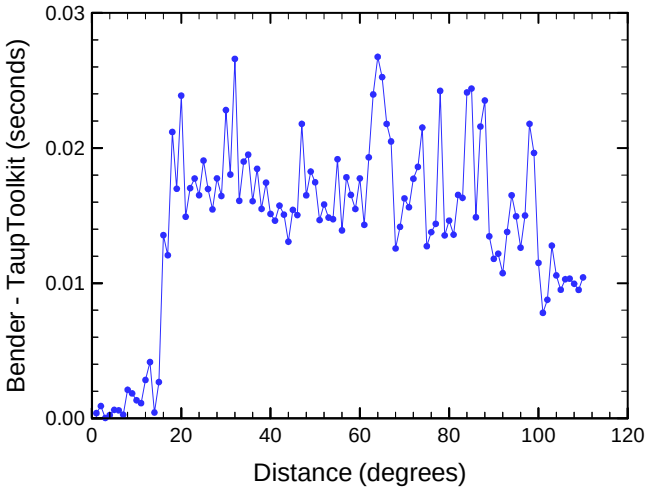

Figure 7. Difference in travel time computed by Bender and Taup Toolkit through the AK135 velocity model.

As with all finite-difference eikonal solvers, the FMM algorithm works by following a wavefront as it moves across a volume of grid points, updating the travel times in the grid according to the eikonal differential equation, using a second-order finite-difference scheme. We chose to use FMM for our comparison because it has a number of important features that make it well suited for making calculations in the regional-to-teleseismic distance ranges that we are interested in. First, the propagation grid is in spherical coordinates rather than Cartesian coordinates, so the sphericity of the Earth can be more readily represented. Second, interfaces are explicitly represented in the FMM grid, regardless of the propagation grid spacing. Thus, a finer propagation grid is not necessary to capture discontinuities with topography, like the Moho. Third, FMM allows calculation of secondary phases, so it can be used for non–first-arrival phases. Finally, finer grid spacing can be used near the source to better capture the highly curved wavefront and hence improve accuracy without drastically increasing the overall number of nodes.

For purposes of comparing travel times computed using Bender with those computed using FMM, we chose station NIL located in Nilore, Pakistan, at latitude 33.6506 N and longitude 72.2686 E. Even though the station is 0.629 km above sea level, we set the elevation to sea level for these calculations in order to avoid having to compute elevation corrections for the FMM results. Next, we specified a 40º × 40º grid of sources extending from 53º to 93º E longitude and 14º to 54º N latitude, with 0.25º grid spacing in both directions. All sources were positioned at 10 km below sea level. We computed travel times from these sources to the position of station NIL using both Bender and FMM. With Bender, it was possible to compute point-to-point travel times for these source-receiver pairs directly, but with FMM we had to first construct a 3D grid that extended from sea level to a depth of 1000 km in order to ensure that the depth of the grid exceeded the deepest bottoming depth of any rays we were interested in. In addition, the FMM grid had to be denser than 0.25º × 0.25º in order to achieve sufficient accuracy. To test the accuracy of the FMM results, we constructed two finite-difference grids, one 0.125º × 0.125º × 10 km and the other 0.0625º × 0.0625º × 5 km. Due to computer-memory limitations, we had to break the 3D grid into four quadrants, run FMM on each quadrant separately, recombine the results into a single grid, and finally subsample the FMM grids at the points of the 2D Bender grid. The difference in travel time between FMM and Bender, for the two different FMM grid resolutions, is illustrated in Figure 8. The difference in travel time decreased as a function of FMM grid resolution, and FMM travel time was virtually always greater than Bender travel time. From these observations we conclude that the Bender travel times are likely a better reflection of the actual travel time through the Earth model used in the calculations. It is entirely possible that FMM travel times would have been reduced, and approached the Bender travel times, had we been able to improve the resolution of the FMM grid even further. We were prevented from doing that by computer-memory limitations

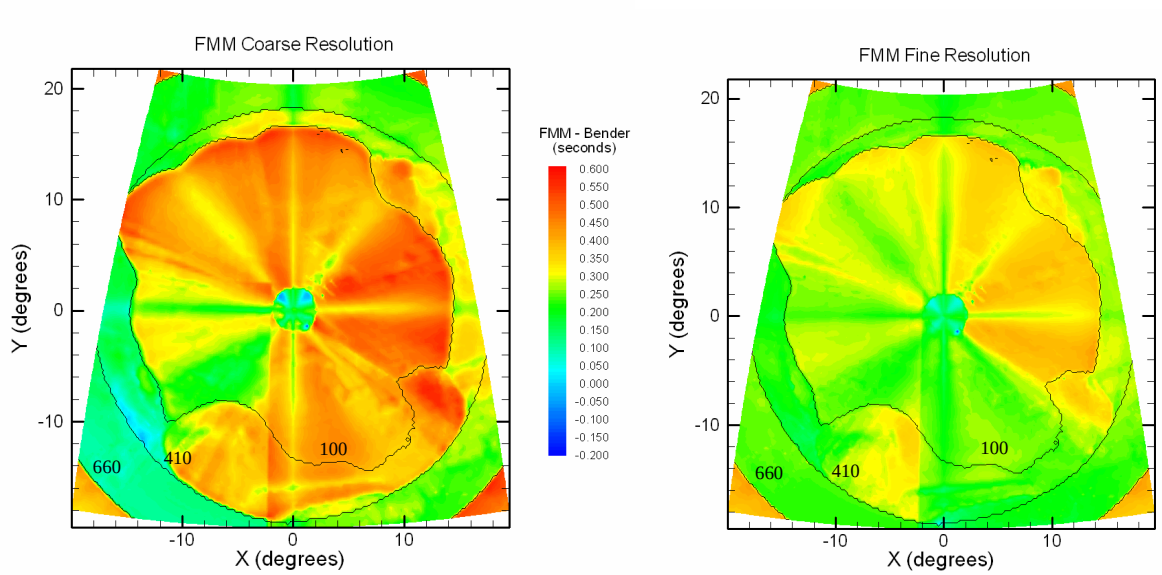

Figure 8. FMM travel time minus Bender travel time for a 40º × 40º grid surrounding station NIL. On the left, the FMM travel times were computed on a 0.125º × 0.125º × 10 km grid; on the right, they were computed on a 0.0625º × 0.0625º × 5 km grid. Black contour lines indicate positions of sources where rays bottomed at depths of 100 km, 440 km, and 660 km, as determined by Bender.

Distributed Computing

The enhancements we have made to the pseudo-bending algorithm of Um and Thurber (1987), as modified by Zhao et al. (1992), have made it more robust and accurate but have also made it more computationally expensive. Our implementation typically requires approximately 0.5 seconds to compute one travel time on a single computer processor. To mitigate these negative performance impacts, we have implemented the software, which is written entirely in the Java programming language, in a distributed computing environment, using the Java Parallel Processing Framework (JPPF; www.jppf.org). This technology makes it fairly straightforward to run many travel-time calculations simultaneously on all available PC, Mac, Unix, and Linux computers. We are currently running our software on a cluster of nine 16-processor PC computers running the 64-bit Windows Server 2003 operating system. Combined with other PCs, Linux boxes, and Sun workstations, our system has almost 200 processors available for calculating travel times.

CONCLUSIONS

We have implemented the pseudo-bending algorithm of Um and Thurber (1987), as modified by Zhao et al. (1992), for computing predicted travel times through 3D velocity models. We have modified Zhao's method of handling discontinuities by implementing a 2D minimization algorithm that searches for the point on the velocity discontinuity surface where Snell's Law is satisfied. Our implementation also significantly decreases the likelihood that the algorithm will return a ray that represents a local minimum by computing rays that bottom in many different specified layers in the model and returning the ray that yields the smallest travel time. We have validated our algorithm by comparing it with the TaupToolkit software (Crotwell et al., 1999) for radially symmetric 1D Earth models. We have also compared our results with travel times computed with the FMM finite-difference calculator (De Kool et al., 2006) and demonstrated that the Bender yields superior results with substantially fewer computer resources.

We are currently developing improved velocity models of the Earth using a tomographic inversion system that uses our Bender software as the forward travel-time calculator. Preliminary results for a study in southcentral Asia are reported in Young et al. (2008, these Proceedings).

ACKNOWLEDGEMENTS

We thank Marthijn de Kool for his help in getting the FMM code running on our computers, and the GNEMRD researchers at Los Alamos National Laboratory and Lawrence Livermore National Laboratory for providing us with their a priori 3D geophysical model.

REFERENCES

Ballard, S., Hipp, J., and C. Young (2008). Robust, extensible representation of complex earth models for use in seismological software systems, these Proceedings.

Begnaud, M. L., C. A. Rowe, and L. K. Steck (2004). Validating three-dimensional velocity models in China and East-Asia for use in regional seismic event location, EOS *Trans. AGU*, Fall Meet. Suppl.

Crotwell, H. P., T. J. Owens, and J. Ritsema (1999). The TauP toolkit: Flexible seismic travel-time and ray-path utilities, *Seism. Res. Lett*. 70: 154–160.

De Kool, M., N. Rawlinson, and M. Sambridge (2006). A practical grid based method for tracking multiple refraction and reflection phases in 3D heterogeneous media, *Geophys. J. Int*. 167: 253–270.

Flanagan, M. P., S. C. Myers, and K. D. Koper (2007). Regional travel-time uncertainty and seismic location improvement using a three-dimensional a priori velocity model, *Bull. Seism. Soc. Am.* 97: 804–825.

Hole, J. A. and B. C. Zelt (1995). 3D finite-difference reflection traveltimes, *Geophys. J. Int.* 121: 427–434.

Kennett, B. L. N., E. R. Engdahl, and R. Buland (1995). Constraints on seismic velocities in the Earth from traveltimes, *Geophys. J. Int*. 122: 108–124.

Koketsu, K. and S. Sekine (1998). Pseudo-bending method for three-dimensional seismic ray tracing in a spherical earth with discontinuities, *Geophys. J. Int.* 132: 339–46.

Laske, G. and T. G. Masters (1997). A global digital map of sediment thickness, *EOS Trans. AGU* 78: F483.

Menke, W. Case studies of seismic tomography and earthquake location in a regional context, http://www.ldeo.columbia.edu/users/menke/R3DPAPER/r3dpaper.pdf.

Nataf, H. C. and Y. Ricard (2004). 3SMAC: An a priori tomographic model of the upper mantle based on geophysical modeling, *Phys. Earth Planet. Int*. 95: 101–122.

Pasyanos, M. E., W. R. Walter, M. P. Flanagan, P. Goldstein, and J. Bhattacharyya (2004). Building and testing an a priori geophysical model for Western Eurasia and North Africa, *Pure Appl. Geophys*. 161: 234–281.

Podvin, P. and I. Lecomte (1991). Finite difference computation of traveltimes in very contrasted velocity models: A massively parallel approach and its associated tools, *Geophys. J. Int.* 105: 271–284.

Rawlinson, N. and M. Sambridge (2004a). Multiple reflection and transmission phases in complex layered media using a multistage fast marching method, *Geophysics* 5: 1338–1350.

Rawlinson, N. and M. Sambridge (2004b). Wave front evolution in strongly heterogeneous layered media using the fast marching method, *Geophys. J. Int*. 156: 631–647.

Um, J. and C. H. Thurber (1987). A fast algorithm for two-point seismic ray tracing, *Bull. Seismol. Soc. Am*. 77: 972–986.

Vidale, J. E. (1988). Finite-difference calculations of traveltimes, *Bull. Seism. Soc. Am*. 78: 2062–2076.

Vidale, J. E. (1990). Finite-difference calculations of traveltimes in three dimensions, *Geophysics* 55: 521–526.

Young, C. J., S. Ballard, J. R. Hipp, M. C. Chang, G. T. Barker, M. L. Begnaud, W. S. Phillips, L. K. Steck, and C. A. Rowe (2008). A 3D tomographic model of south central Asia based on Pn travel times from GT events, these Proceedings.

Zhao, D., A. Hasegawa, and S. Horiuchi (1992). Tomographic imaging of P and S wave velocity structure beneath northwestern Japan. *JGR* 97: B13, 19, 909–19,928.